The Astrophysical Journal Letters, 841:L22 (8pp), 2017 June 1 https://doi.org/10.3847/2041-8213/aa70e9
© 2017. The American Astronomical Society. All rights reserved.

CANDELS Sheds Light on the Environmental Quenching of Low-mass Galaxies

Yicheng Guo[1], Eric F. Bell[2], Yu Lu[3], David C. Koo[1], S. M. Faber[1], Anton M. Koekemoer[4], Peter Kurczynski[5], Seong-Kook Lee[6], Casey Papovich[7,8], Zhu Chen[9], Avishai Dekel[10], Henry C. Ferguson[4], Adriano Fontana[11], Mauro Giavalisco[12], Dale D. Kocevski[13], Hooshang Nayyeri[14], Pablo G. Pérez-González[15], Janine Pforr[16,17], Aldo Rodríguez-Puebla[18], and Paola Santini[11]
[1] UCO/Lick Observatory, Department of Astronomy and Astrophysics, University of California, Santa Cruz, CA, USA; ycguo@ucolick.org
[2] Department of Astronomy, University of Michigan, Ann Arbor, MI, USA
[3] Observatories, Carnegie Institution for Science, Pasadena, CA, USA
[4] Space Telescope Science Institute, Baltimore, MD, USA
[5] Department of Physics and Astronomy, Rutgers University, Piscataway, NJ, USA
[6] Center for the Exploration of the Origin of the Universe, Department of Physics and Astronomy, Seoul National University, Seoul, Korea
[7] Department of Physics and Astronomy, Texas A&M University, College Station, TX, USA
[8] George P. and Cynthia Woods Mitchell Institute for Fundamental Physics and Astronomy, Texas A&M University, College Station, TX, USA
[9] Shanghai Key Lab for Astrophysics, Shanghai Normal University, 100 Guilin Road, Shanghai 200234, China
[10] Center for Astrophysics and Planetary Science, Racah Institute of Physics, The Hebrew University, Jerusalem, Israel
[11] INAF-Osservatorio Astronomico di Roma, Via Frascati 33, Monte Porzio Catone, I-00078 Rome, Italy
[12] Department of Astronomy, University of Massachusetts, Amherst, MA, USA
[13] Colby College, Waterville, ME, USA
[14] Department of Physics and Astronomy, University of California, Irvine, CA, USA
[15] Departamento de Astrofísica, Facultad de CC. Físicas, Universidad Complutense de Madrid, E-28040 Madrid, Spain
[16] Aix Marseille Université, CNRS, LAM (Laboratoire d'Astrophysique de Marseille) UMR 7326, F-13388, Marseille, France
[17] ESA/ESTEC, Noordwijk, The Netherlands
[18] Instituto de Astronomía, Universidad Nacional Autónoma de México, A. P. 70-264, 04510 México, D.F., México
Received 2016 November 21; revised 2017 April 24; accepted 2017 May 2; published 2017 May 24

Abstract

We investigate the environmental quenching of galaxies, especially those with stellar masses (M_*) $< 10^{9.5}\,M_\odot$, beyond the local universe. Essentially all local low-mass quenched galaxies (QGs) are believed to live close to massive central galaxies, which is a demonstration of environmental quenching. We use CANDELS data to test whether or not such a dwarf QG-massive central galaxy connection exists beyond the local universe. For this purpose, we only need a statistically representative, rather than complete, sample of low-mass galaxies, which enables our study to $z \gtrsim 1.5$. For each low-mass galaxy, we measure the projected distance ($d_{\rm proj}$) to its nearest massive neighbor ($M_* > 10^{10.5}\,M_\odot$) within a redshift range. At a given z and M_*, the environmental quenching effect is considered to be observed if the $d_{\rm proj}$ distribution of QGs ($d_{\rm proj}^{Q}$) is significantly skewed toward lower values than that of star-forming galaxies ($d_{\rm proj}^{\rm SF}$). For galaxies with $10^8\,M_\odot < M_* < 10^{10}\,M_\odot$, such a difference between $d_{\rm proj}^{Q}$ and $d_{\rm proj}^{\rm SF}$ is detected up to $z \sim 1$. Also, about 10% of the quenched galaxies in our sample are located between two and four virial radii ($R_{\rm Vir}$) of the massive halos. The median projected distance from low-mass QGs to their massive neighbors, $d_{\rm proj}^{Q}/R_{\rm Vir}$, decreases with satellite M_* at $M_* \lesssim 10^{9.5}\,M_\odot$, but increases with satellite M_* at $M_* \gtrsim 10^{9.5}\,M_\odot$. This trend suggests a smooth, if any, transition of the quenching timescale around $M_* \sim 10^{9.5}\,M_\odot$ at $0.5 < z < 1.0$.

Key words: galaxies: dwarf – galaxies: evolution – galaxies: star formation – galaxies: statistics

1. Introduction

Environmental effects are believed to be the primary process of ceasing star formation in low-mass galaxies with stellar masses (M_*) lower than $10^{9.5}\,M_\odot$ (or dwarf galaxies). Field low-mass galaxies may temporarily quench their star formation through supernova feedback, but new gas accretion and recycling would induce new starbursts with periods of tens of megayears (e.g., Guo et al. 2016; Sparre et al. 2017). Geha et al. (2012, hereafter G12) found that the quenched fraction of galaxies with $M_* < 10^9\,M_\odot$ drops rapidly as a function of distance to massive host galaxies and that essentially all local field galaxies in this mass regime are forming stars.

The environmental quenching of low-mass galaxies beyond the local universe, however, is rarely investigated because of these galaxies' faint luminosity. Most studies (e.g., G12; Quadri et al. 2012; Tal et al. 2013, 2014; Balogh et al. 2016; Kawinwanichakij et al. 2016; Fossati et al. 2017, etc.) start from central galaxies and measure the quenched fraction of their satellites. This method requires a complete sample of satellites, which limits these studies to the local universe and/or to intermediate-mass ($M_* \gtrsim 10^{9.5}\,M_\odot$) satellites.

In this letter, we use CANDELS data (Grogin et al. 2011; Koekemoer et al. 2011) to detect the effects of environmental quenching beyond $z \sim 1$. Our approach is different from but complementary to other studies. We start from the "victims"—quenched dwarf galaxies—and search for their massive neighbors, which are tracers of massive dark matter halos.

The concept of our approach is simple—if environmental effects are solely responsible for quenching all dwarf galaxies, all low-mass quenched galaxies (QGs) should live close to a massive central galaxy in a massive halo. In contrast, star-forming galaxies (SFGs) can live far away from massive dark matter halos. Therefore, on average, QGs should have systematically shorter distances to their massive neighbors than SFGs should. This systematic difference between the two populations is evidence of the dwarf QG-massive central galaxy connection and therefore a demonstration of environmental quenching. Because our goal is to investigate whether or not such a dwarf

QG-massive central connection has been established, we only need to detect a statistically meaningful signal, rather than to find all signals, to rule out the null hypothesis of no environmental effects. This advantage allows us to use an incomplete dwarf sample to study this topic beyond the local universe.

We adopt a flat ΛCDM cosmology with $\Omega_m = 0.3$, $\Omega_\Lambda = 0.7$, and the Hubble constant $h \equiv H_0/100\ \mathrm{km\ s^{-1}\ Mpc^{-1}} = 0.70$. We use the AB magnitude scale (Oke 1974) and a Chabrier (2003) IMF.

2. Data

We use the photometric redshift (photo-z), M_*, and rest-frame color catalogs of four CANDELS fields: GOODS-S (Guo et al. 2013), UDS (Galametz et al. 2013), GOODS-N (G. Barro et al. 2017, in preparation) and COSMOS (Nayyeri et al. 2017).

The photo-z measurement is described in Dahlen et al. (2013). For GOODS-S galaxies at $0.5 < z < 2.0$ and $H < 26$ AB, the 1σ scatter of $|\Delta z|/(1+z)$ is 0.026 and the outlier fraction (defined as $|\Delta z|/(1+z) > 0.1$) is 8.3%. We also divide the test sample into low-mass ($M_* < 10^9\,M_\odot$) and massive ($M_* > 10^9\,M_\odot$) sub-samples. The 1σ scatter and outlier fraction of the low-mass (and massive) sub-sample are 0.033 (0.024) and 13.7% (7.2%).

The M_* measurement is described in Santini et al. (2015), where each galaxy is fit by 12 SED-fitting codes with different combinations of synthetic stellar population models, star formation histories, fitting methods, etc. For each galaxy, we use the median of the 12 best-fit M_* as its M_*. The typical uncertainty of M_* measurement is ∼0.15 dex. Rest-frame colors are measured using EAZY (Brammer et al. 2008).

3. Method

3.1. Sample Selection

Our sample consists of sources with F160W $H < 26$ AB, PHOTFLAG = 0 (no suspicious photometry), and SExtractor CLASS_STAR < 0.8. The magnitude limit of $H = 26$ AB is approximately the 50% completeness limit of CANDELS wide regions (Guo et al. 2013) and it is corresponding to a galaxy of $M_* \sim 10^8\,M_\odot$ at $z \sim 0.5$ with a single stellar population that is 5 Gyr old. We divided the whole sample into different z and M_* bins: $z = 0.5$–2 with $\Delta z = 0.25$ and $\log(M_*) = 8.0$–10.5 with $\Delta \log(M_*) = 0.5$.

In each (z, M_*) bin, we use the UVJ diagram (Williams et al. 2009; Muzzin et al. 2013) to select QGs and SFGs. To avoid the contamination of misidentified stars and sources with suspicious colors, we add one criterion to refine the quenching region (the diagonal light brown line within the original UVJ quenched region in Figures 1(a)–3(a)). This extra criterion may exclude some very compact QGs (Barro et al. 2013), but since our goal is to obtain a clean and statistically meaningful sample rather than a complete one, such exclusion is necessary and does not affect our results.

For SFGs, instead of using all galaxies in the UVJ star-forming region, we measure the median and $\pm 1.5\sigma$ level of the star-forming locus (calculated in the directions parallel and perpendicular to the reddening vector) and use them as the selection boundary. The selected SFGs are plotted as blue points in Figures 1(a)–3(a). Again, although many galaxies in the original UVJ star-forming locus are excluded, we aim at constructing a clean rather than complete sample.

3.2. Detecting Environmental Quenching Effects

For each low-mass galaxy, we search for its nearest massive neighbor in the sky (projected distance). The massive sample is selected to have CLASS_STAR < 0.8, PHOTFLAG = 0, $M_*^{\mathrm{massive}} > 10^{10.5}\,M_\odot$, and $M_*^{\mathrm{massive}} > M_*^{\mathrm{low\text{-}mass}} + 0.5$ dex.[19] The redshift range of the massive sample is limited to $|z_{\mathrm{massive}} - z_{\mathrm{low\text{-}mass}}|/(1 + z_{\mathrm{low\text{-}mass}}) < 0.10$, which is about 3σ of our photo-z accuracy. We calculate the projected distances between the low-mass galaxy and all selected massive galaxies. The massive galaxy with the smallest projected distance is chosen as the central galaxy of the low-mass galaxy. We use d_{proj} to denote this smallest projected distance.

Because of projection effects, a massive neighbor found through this method may not be the real massive galaxy whose dark matter halo was responsible for quenching the low-mass galaxy. But if environmental effects are the primary way of quenching a population of low-mass galaxies, statistically, QGs should be located closer to massive companions than SFGs should. As a result, the d_{proj} distribution of a quenched population (d_{proj}^{Q}) should be skewed toward lower values than that of SFGs ($d_{\mathrm{proj}}^{\mathrm{SF}}$).

Many studies (e.g., Scoville et al. 2013; Davies et al. 2016) used the local overdensity field constructed by Voronoi tessellation or the nearest neighbor method to measure environments. Since the local overdensity of a satellite galaxy is correlated with d_{proj}, our method is similar to those using a density field. While our simple method provides necessary information to test the "whether or not" question of our particular interest, future work with the density field approach could provide more accurate and detailed measurements of environmental quenching.

We test whether d_{proj}^{Q} is systematically and significantly smaller than $d_{\mathrm{proj}}^{\mathrm{SF}}$ in each (z, M_*) bin. Because in most (z, M_*) bins, the number of QGs is much smaller than that of SFGs, the small number statistics needs to be taken into account. In each of these bins, we randomly draw a sub-sample of the SFGs to match the number of the QGs and calculate the median, probability distribution function (PDF), and cumulative distribution functions (CDF) of d_{proj} of the sub-sample ($d_{\mathrm{proj}}^{\mathrm{SF,sub}}$). We repeat this bootstrapping sampling 3000 times, obtaining 3000 distributions of $d_{\mathrm{proj}}^{\mathrm{SF,sub}}$. To exclude the null hypothesis, we ask the median d_{proj}^{Q} to be 3σ smaller than the median of $d_{\mathrm{proj}}^{\mathrm{SF,sub}}$.

Figures 1(b)–3(b) show some examples of our results. The (z, M_*) bins labeled with $\geqslant 3\sigma$ values (i.e., median d_{proj}^{Q} is 3σ smaller than median $d_{\mathrm{proj}}^{\mathrm{SF,sub}}$) are considered to have an established quenching–environment connection. In contrast, bins with $<3\sigma$ values cannot rule out the null hypothesis of the two populations having the same d_{proj} distributions with 3σ confidence.

[19] The last requirement only affects galaxies with $10^{10}\,M_\odot < M_*^{\mathrm{low\text{-}mass}} < 10^{10.5}\,M_\odot$. The M_*^{massive} threshold of our massive sample corresponds to dark matter halos of $M_{\mathrm{halo}} \gtrsim 10^{12}\,M_\odot$. Since the M_*–M_{halo} relation evolves little with redshift in this mass regime (Behroozi et al. 2013), our choice of a fixed M_*^{massive} threshold at different redshifts allows us to investigate the environmental effects of similar M_{halo} at different cosmic times.

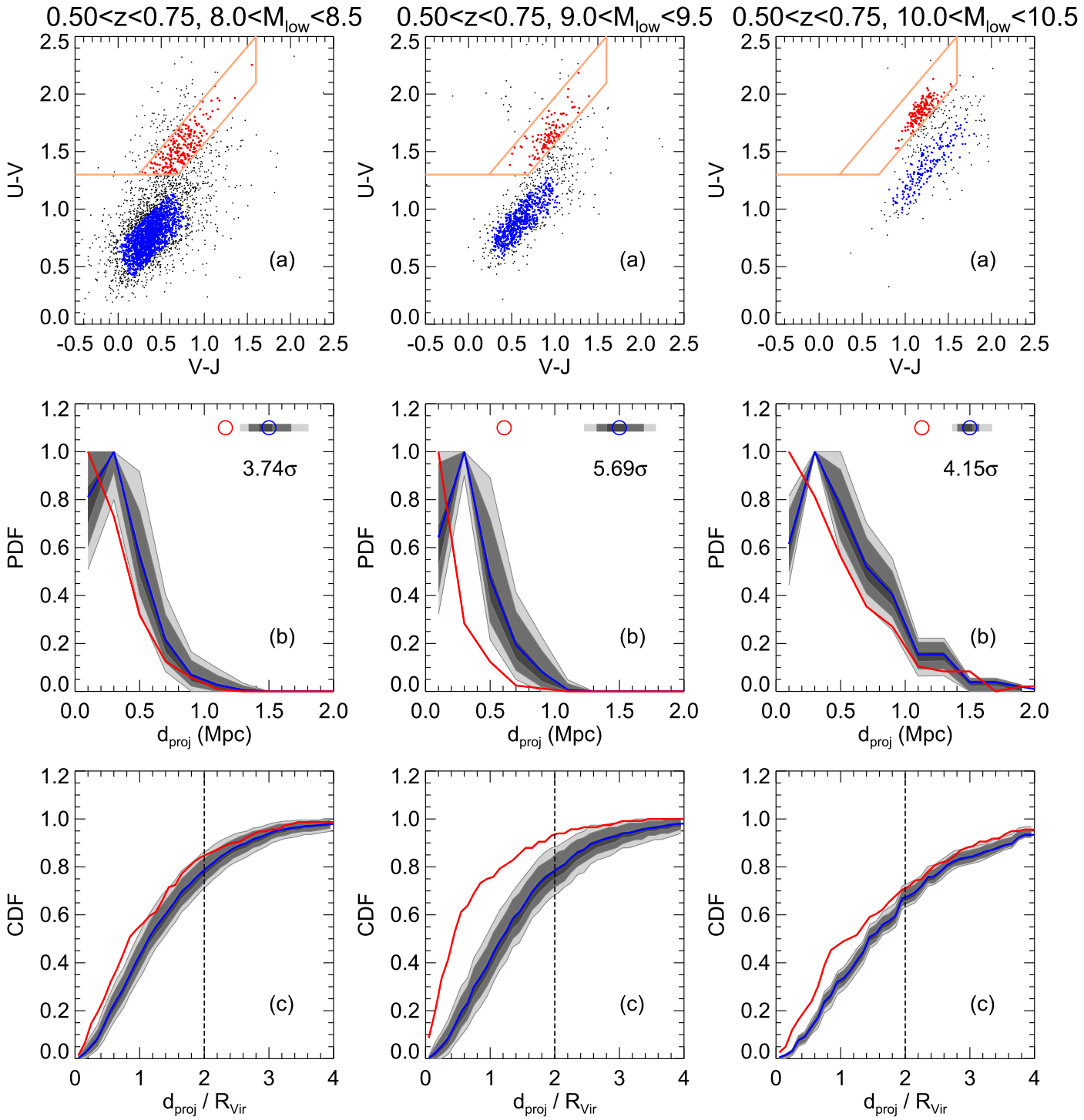


Figure 1. Examples of sample selection and environment measurement. Each column shows a given (z, M_*) bin as the title shows. In each column, Panel (a) shows the selected QGs (red) and SFGs (blue) in the UVJ diagram. Black dots show all galaxies (with $H_{F160W} < 26$ and CLASS_STAR < 0.8) in this bin. Panel (b) shows the PDFs of $d_{\rm proj}$ of the QGs (red) and SFGs (blue) galaxies. The dark, medium, and light gray regions show the 1σ, 2σ, and 3σ levels of 3000 times of bootstrapping of SFGs to match the number of QGs. The red and blue circles show the medians of $d_{\rm proj}$ of the QGs and SFGs. The gray bar shows the 1σ (dark), 2σ (medium), and 3σ (light) levels of the medians of the bootstrapping. To show the difference clearly, all median values are normalized so that the median of the SFGs (blue circle) is equal to 1.5 Mpc. The number below the gray bar shows the confidence level to which the null hypothesis that the QGs (red) and SFGs (blue) have the same $d_{\rm proj}$ medians is ruled out. Panel (c) shows the CDFs of $d_{\rm proj}$ of the QGs (red) and SFGs (blue) normalized by $R_{\rm Vir}$ of the halos of their massive neighbors. The dark, medium, and light gray regions show the 1σ, 2σ, and 3σ levels of the bootstrapping. All columns in this figure are at $0.5 < z < 0.75$.

4. Results

Figure 4(a) shows the deviation from $d_{\rm proj}^{Q}$ to $d_{\rm proj}^{\rm SF,sub}$ in each (z, M_*) bin. Our criterion of environmental quenching being observed is that the median of $d_{\rm proj}^{Q}$ is 3σ smaller than that of $d_{\rm proj}^{\rm SF,sub}$. For galaxies with $10^8\,M_\odot < M_* < 10^{10}\,M_\odot$, such a quenching–environment connection is observed up to $z \sim 1$, as shown by the larger-than-3σ deviations. This result is consistent with the quick emergence of low-mass QGs from the

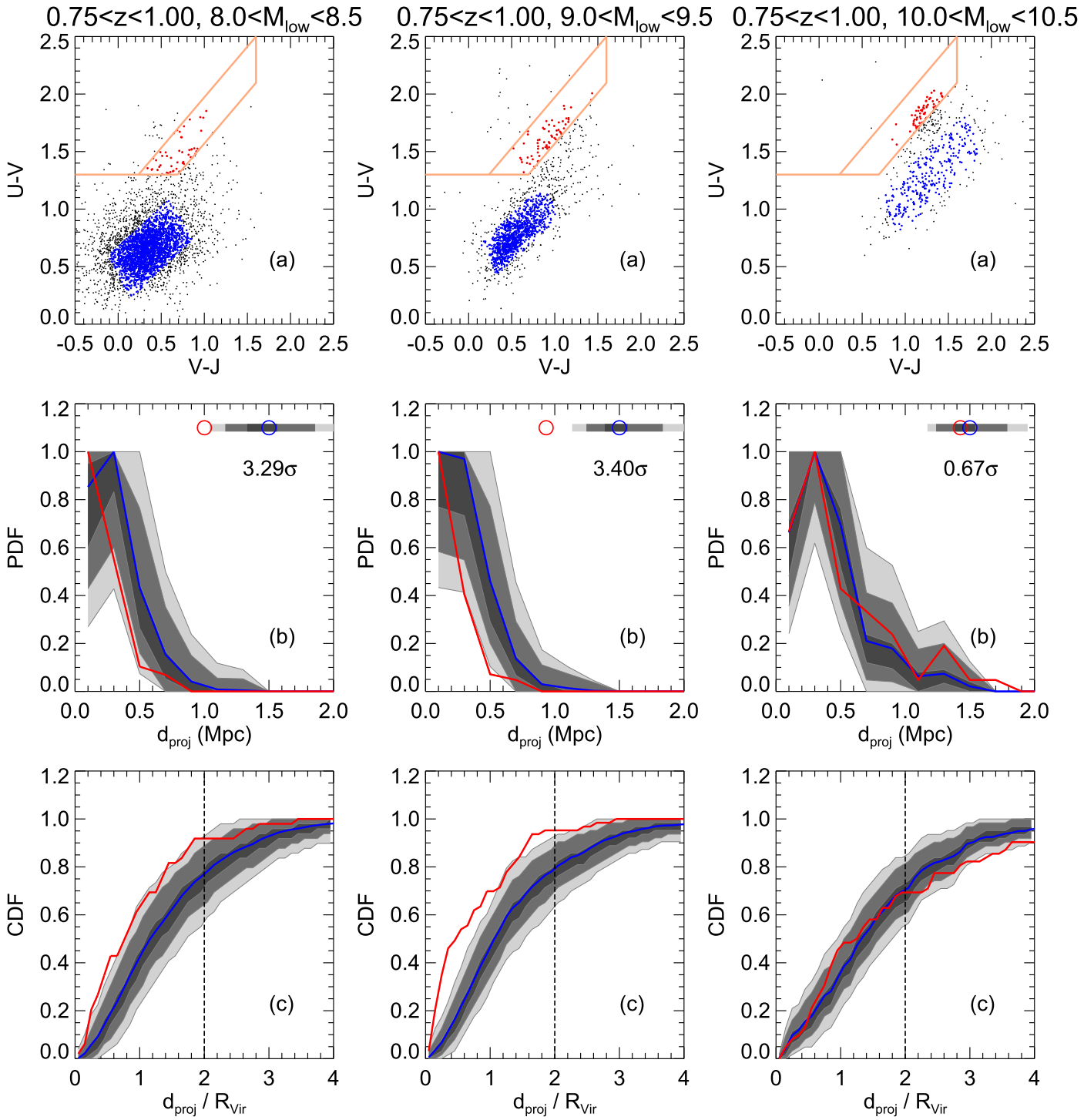


Figure 2. Same as Figure 1, but showing three M_* bins at $0.75 < z < 1.00$.

measurement of stellar mass functions at $z \sim 1$ (e.g., Huang et al. 2013; Ilbert et al. 2013). For galaxies with $10^{10.0}\,M_\odot < M_* < 10^{10.5}\,M_\odot$, the connection was established at a lower redshift.

For those (z, M_*) bins with $<3\sigma$ deviation, we cannot rule out the null hypothesis of QGs and SFGs having the same $d_{\rm proj}$ distributions with more than 3σ confidence. This may imply that the quenching–environment connection has not been established in these bins. This interpretation is at least consistent with some other studies for massive galaxies ($M_* > 10^{10}\,M_\odot$), which claimed that massive quiescent galaxies at $z > 1$ are not necessarily located in high-density environments (e.g., Darvish et al. 2015, 2016; Lin et al. 2016). For lower-mass galaxies at $z \gtrsim 1.5$, however, due to projection effects or small number statistics, our method may have failed to detect existing quenching–environment connections.

5. Discussion

5.1. Spatial Distribution of Quenched Galaxies

G12 found that 87% (and 97%) of dwarf QGs in their SDSS sample are within 2 $R_{\rm Vir}$ (and 4 $R_{\rm Vir}$) of a massive host galaxy. We find similar results in our sample at $0.5 < z < 1.0$ (Figure 4(b)).

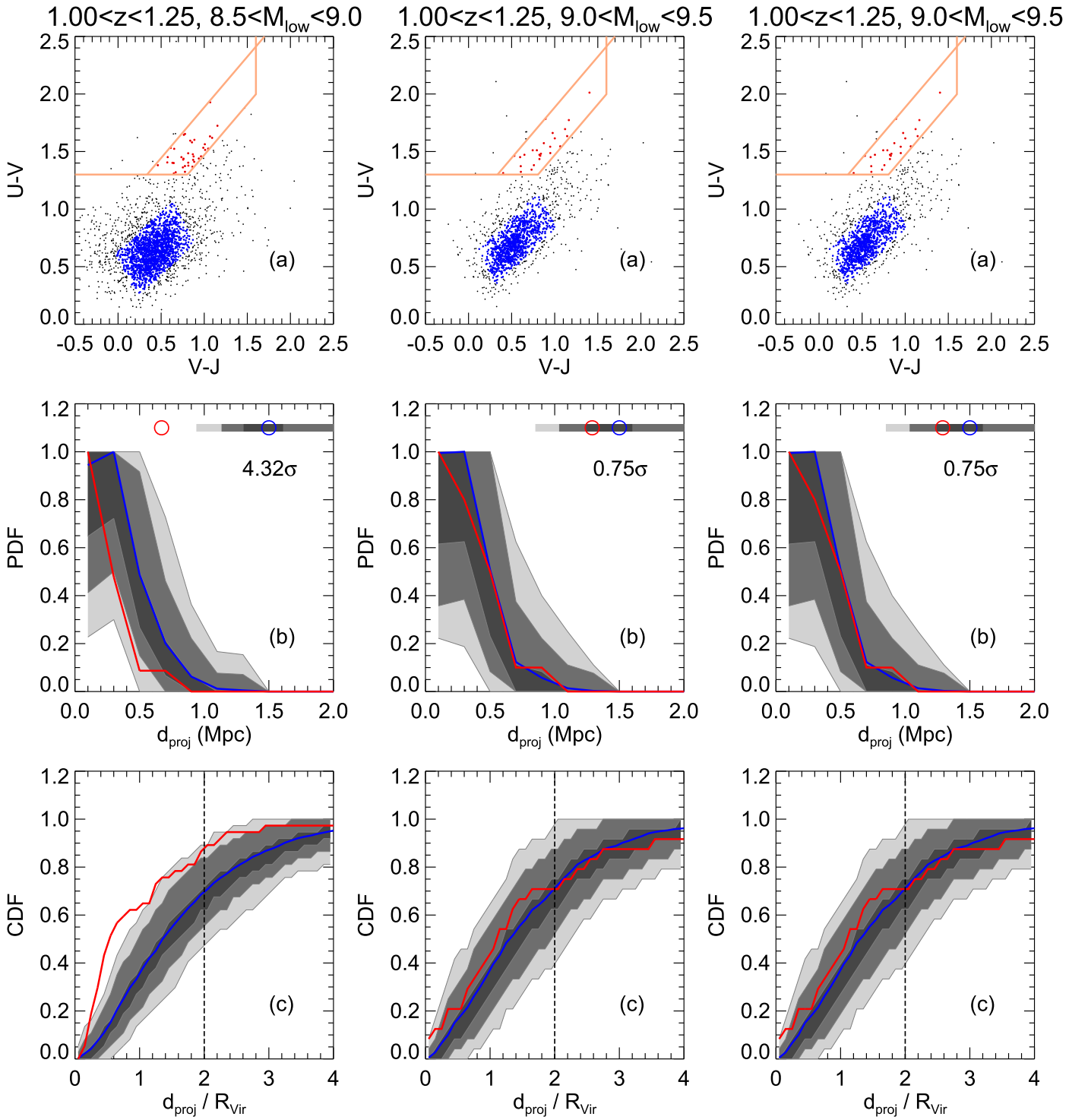


Figure 3. Same as Figure 1, but showing three M_* bins at $1.00 < z < 1.25$.

About 90% of the QGs below $10^{10}\,M_\odot$ in our sample are within 2 $R_{\rm Vir}$. The fraction drops quickly to about 70% for galaxies above $10^{10}\,M_\odot$. To calculate $R_{\rm Vir}$, we first use the M_*–$M_{\rm halo}$ relation of Behroozi et al. (2013) to obtain $M_{\rm halo}$ ($M_{\rm vir}$) of the massive neighbors. Then, we derive $R_{\rm Vir}$ through $M_{\rm vir}(z) = \frac{4\pi}{3}\Delta_{\rm c}(z)\rho_{\rm crit}(z)R_{\rm vir}(z)^3$, where $\rho_{\rm crit}(z)$ is the critical density of the universe at z, and $\Delta_{\rm c}(z)$ is calculated by following Bryan & Norman (1998).

SFGs in our sample are also almost within 4 $R_{\rm Vir}$. This could be a projection effect. Since we search for massive neighbors within a long line-of-sight distance ($|\Delta z|/(1+z) < 0.10$), an SFG has a high chance of being located within the projected 4 $R_{\rm Vir}$ of a massive galaxy, even though the massive galaxy is not its real central galaxy. In contrast, with a more accurate redshift measurement, G12 found that only ~50% of the $z \sim 0$ SFGs are within 4 $R_{\rm Vir}$, suggesting that a large fraction of SFGs are

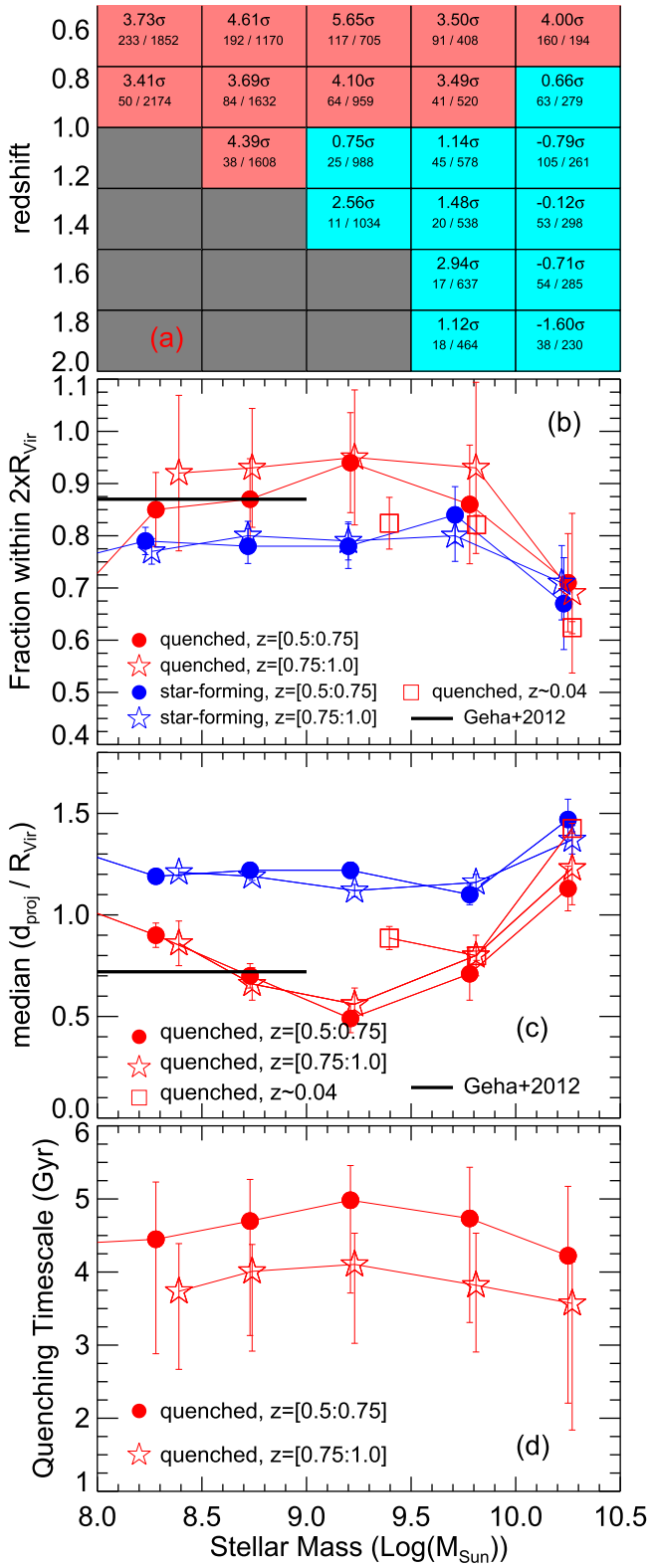


Figure 4. Panel (a): statistics of the quenching–environment connection. In each (z, M_*) bin, the deviation between the medians of $d_{\rm proj}^{Q}$ and $d_{\rm proj}^{\rm SF,sub}$ is the upper number, while the numbers of the QGs and SFGs are the two lower numbers. We choose the deviation $\geqslant 3\sigma$ as the threshold of the quenching–environment connection being observed. All such bins are red, while others with the deviation $<3\sigma$ are cyan. Gray bins cannot be accessed by our current data set. Panel (b): fraction of a population of galaxies within 2 $R_{\rm Vir}$ of massive halos. Different symbols show different populations. Panel (c): median $d_{\rm proj}/R_{\rm Vir}$ of different samples. Panel (d): inferred quenching timescales in two redshift bins. The colors and symbols in Panels (b)–(d) are the same.

intrinsically outside 4 $R_{\rm Vir}$. QGs in our sample may suffer from the same projection effect. However, as discussed in Section 3.2, this effect would not affect our *statistical* results.

A non-negligible fraction (10%) of low-mass QGs are located between 2 and 4 $R_{\rm Vir}$. They are likely central galaxies quenched by mechanisms not related to environment, e.g., AGNs and stellar feedback. They, however, may also be evidence for quenching processes acting at large distances of massive halos (e.g., Cen 2014). Y. Lu et al. (2017, in preparation) found that, to match the observed M_* and stellar-phase metallicity simultaneously, gas accretion of Milky Way (MW) satellite galaxies need to be largely reduced way before they fall into $R_{\rm Vir}$ of the MW halo, possibly by heating up the intergalactic medium in the MW halo vicinity to 10^5 K. Alternatively, Slater & Bell (2013) used simulations to show that environmental effects are prominent out to 2–3 $R_{\rm Vir}$: satellites with very distant apocenters can be quenched by tidal stripping and ram pressure stripping following a close passage to the host galaxy.

We also extend the local results of G12 to higher M_* by repeating our measurements on the SDSS sample of Rodríguez-Puebla et al. (2015). The results (red squares in Figure 4(b)), together with G12, suggest that the fraction of QGs with 2 $R_{\rm Vir}$ has almost no redshift dependence. This constant fraction suggests that, at all redshifts, environment (especially within 2 $R_{\rm Vir}$) dominates the quenching of low-mass galaxies.

We also study the median distance of galaxies to their massive neighbors scaled by $R_{\rm Vir}$ (Figure 4(c)). SFGs have a constant median distance of $\sim$1.3 $R_{\rm Vir}$ over a wide M_* range. QGs are closer to massive neighbors, but their median distance depends on M_*: it decreases from 1 $R_{\rm Vir}$ at $10^8\,M_\odot$ to 0.5 $R_{\rm Vir}$ at $10^{9.5}\,M_\odot$, then increases to $>1R_{\rm Vir}$ at $10^{10.5}\,M_\odot$. Also, we find no significant difference between different redshifts.

5.2. Quenching Timescale

Quenching timescale (T_Q) is important to constrain quenching mechanisms. In the local universe, at $M_* > 10^{10}\,M_\odot$, quenching likely occurs through starvation, whose timescale (4–6 Gyr) is comparable to gas depletion timescales (Fillingham et al. 2015; Peng et al. 2015). At $M_* < 10^8\,M_\odot$, ram pressure stripping is likely the dominant mechanism (Slater & Bell 2014; Fillingham et al. 2015; Weisz et al. 2015). Its timescale (2 Gyr) is much shorter and comparable to the dynamical timescale of the host dark matter halo. The dominant quenching mechanism may change around a characteristic M_*.

To infer T_Q, we assume all galaxies start quenching at 4 $R_{\rm Vir}$. We choose 4 $R_{\rm Vir}$ because G12 shows that beyond 4 $R_{\rm Vir}$ the fraction of QGs is almost zero, while the fraction of SFGs is still high. Theoretically, Cen (2014) also predicted the onset of quenching at a similar large halo distance. Galaxies fall into massive halos while their star formation rates are being reduced. They become fully quenched when they arrive at the observed location. Therefore, T_Q is the time they spent on traveling from 4 $R_{\rm Vir}$ to the observed location with an infall velocity (using circular velocity $V(R) = \sqrt{\frac{GM(<R)}{R}}$ at 2 $R_{\rm Vir}$ as an approximation).

Our method of measuring T_Q is different from most studies in the literature, e.g., Wetzel et al. (2013), Wheeler et al. (2014), Fillingham et al. (2015), Balogh et al. (2016), and Fossati et al. (2017). They used numerical simulations or semi-analytic models to match the basic demographics (e.g., quenched fraction) of QGs. Our method is purely empirical, but relies on the assumptions of the starting and end points (i.e., 4 $R_{\rm Vir}$ and the observed location, respectively) of quenching.

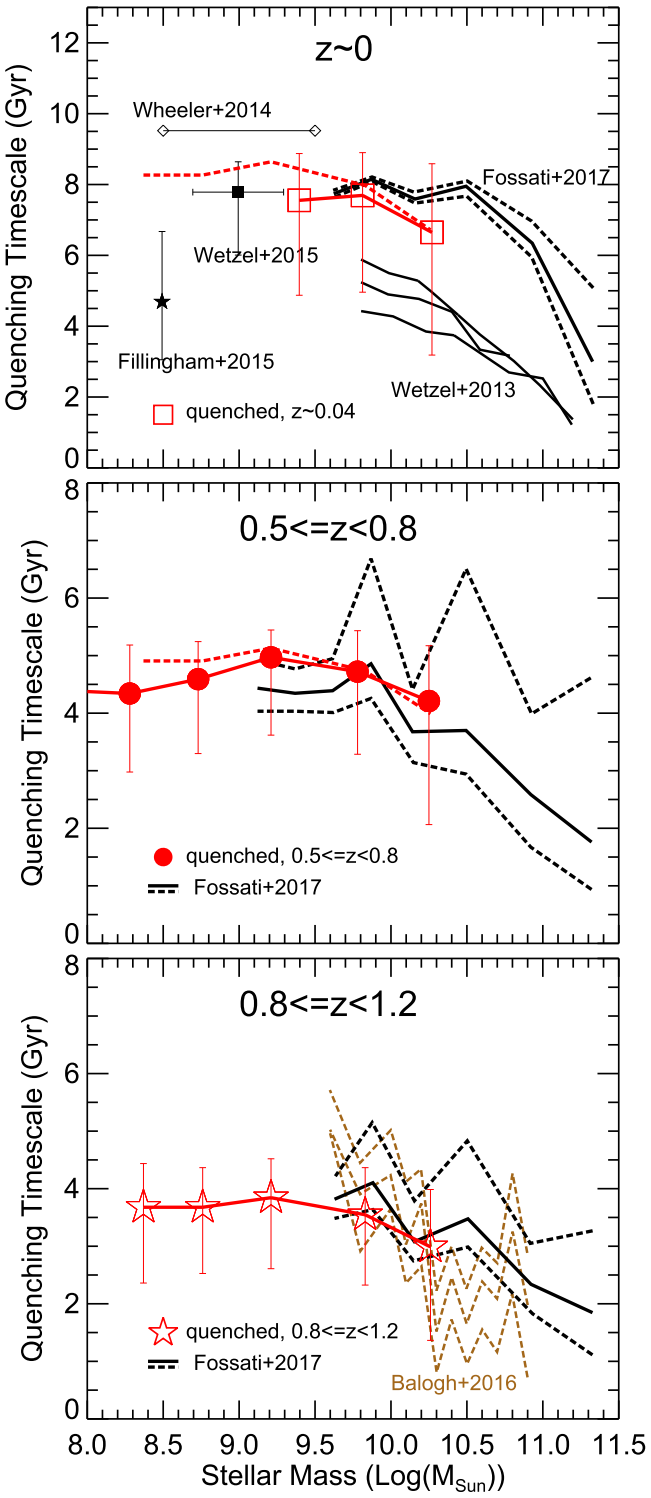


Figure 5. Quenching timescale at different redshifts. The red symbols are calculated by this work, while the black and brown lines and symbols are taken from the literature. The red dashed lines in the first two panels are the solid red line in the third panel (i.e., T_Q at $0.8 \leqslant z < 1.2$) scaled up by $(1+z)^{1.5}$.

Our T_Q definition, however, characterizes the same physical quantity as other methods, i.e., the timescale upon which satellites must quench following infalling into the vicinity of their massive hosts.

The inferred T_Q is shown in Figure 4(d). Overall, the T_Q dependence on M_* is, if any, very weak between 10^8 and $10^{10}\,M_\odot$. Lower-redshift galaxies have longer T_Q, because dynamical timescale decreases with redshift: lower-redshift galaxies need more time to travel the same $d_{\rm proj}^{Q}/R_{\rm Vir}$.

Our measurements show excellent agreement with those of Fossati et al. (2017) and Balogh et al. (2016) at $M_* > 10^{9.5}\,M_\odot$ (Figure 5). Fossati et al. (2017) used 3D-*HST* data (Skelton et al. 2014; Momcheva et al. 2016) to study the environments of galaxies with $M_* \gtrsim 10^{9.5}\,M_\odot$ in CANDELS fields. Agreement with these detailed studies provides an assurance to our method: although built upon simplified assumptions, it is able to catch the basic physical principles of environmental quenching. Moreover, the good agreement also implies that the projection effect discussed in Section 5.1 does not significantly bias our measurement.

Our results, together with the measurements of Fossati et al. (2017) and Balogh et al. (2016), imply a smooth T_Q transition —and hence a quenching mechanism transition—around $M_* \sim 10^{9.5}\,M_\odot$, which is broadly consistent with other studies (e.g., Cybulski et al. 2014; Lee et al. 2015).

At $M_* \gtrsim 10^{10}\,M_\odot$, starvation is likely to be responsible for environmental quenching (Fillingham et al. 2015). Alternatively, however, these galaxies actually could be centrals or recently quenched before becoming satellites. For them, internal mechanisms (e.g., AGNs and star formation feedback) are likely dominating the quenching, as demonstrated by the correlation between star formation and internal structures (e.g., central mass density within 1 kpc discussed in Fang et al. 2013; Barro et al. 2017; Woo et al. 2017).

The quenching mechanisms at $M_* < 10^{9.5}\,M_\odot$ are still uncertain. Our results suggest that T_Q mildly increases with M_* at $0.5 \leqslant z < 0.8$. Other studies of the local universe (e.g., Slater & Bell 2014; Fillingham et al. 2015; Wetzel et al. 2015) suggest a much stronger M_* dependence of T_Q. For example, Fillingham et al. (2016) argued that T_Q drops quickly to ~2 Gyr for galaxies with $M_* \lesssim 10^{8}\,M_\odot$ at $z \sim 0$ because of ram pressure stripping.

At $M_* > 10^{9.5}\,M_\odot$, the redshift dependence of T_Q can be explained by the change of dynamical timescale. We scale up T_Q at $0.8 \leqslant z < 1.2$ by a factor of $(1+z)^{1.5}$ to account for the redshift dependence of the dynamical timescale (see Tinker & Wetzel 2010). This scaled T_Q (red dashed lines in the first two panels of Figure 5) matches the actual T_Q measurements very well at $M_* \gtrsim 10^{9.5}\,M_\odot$. However, it deviates from the T_Q measurements at $M_* < 10^{9.0}\,M_\odot$. At $z \sim 0$ (7 Gyr after $z \sim 1.0$), the scaled T_Q is significantly larger than the T_Q measured by Fillingham et al. (2015). Balogh et al. (2016) also found similar results: at $z \sim 1$, their T_Q of galaxies with $M_* < 10^{10}\,M_\odot$ is longer than the $z \sim 0$ T_Q scaled down by $(1+z)^{1.5}$. Future work is needed to more quantitatively determine the redshift dependence of the T_Q of low-mass galaxies.

6. Conclusions

CANDELS allows us to investigate evidence of environmental quenching of dwarf galaxies beyond the local universe. At $0.5 < z \lesssim 1.0$, we find that for $10^8\,M_\odot < M_* < 10^{10}\,M_\odot$, QGs are significantly closer to their nearest massive companions than SFGs are, demonstrating that environment plays a dominant role in quenching low-mass galaxies. We also find that about 10% of the QGs in our sample are located between two and four $R_{\rm Vir}$ of the massive halos. The median projected distance from the QGs to their massive neighbors ($d_{\rm proj}^{Q}/R_{\rm Vir}$) decreases with satellite M_* at $M_* \lesssim 10^{9.5}\,M_\odot$, but increases with satellite M_* at $M_* \gtrsim 10^{9.5}\,M_\odot$. This trend suggests a

smooth, if any, transition of T_Q around $M_* \sim 10^{9.5} M_\odot$ at $0.5 < z < 1.0$.

Y.G., D.C.K., and S.M.F. acknowledge support from NSF grant AST-0808133. Support for Program HST-AR-13891 and HST-GO-12060 were provided by NASA through a grant from the Space Telescope Science Institute, operated by the Association of Universities for Research in Astronomy, Incorporated, under NASA contract NAS5-26555. Z.C. acknowledges support from NSFC grants 11403016 and 11433003.

References

Balogh, M. L., McGee, S. L., Mok, A., et al. 2016, MNRAS, 456, 4364
Barro, G., Faber, S. M., Koo, D. C., et al. 2017, ApJ, 840, 47
Barro, G., Faber, S. M., Pérez-González, P. G., et al. 2013, ApJ, 765, 104
Behroozi, P. S., Wechsler, R. H., & Conroy, C. 2013, ApJ, 770, 57
Brammer, G. B., van Dokkum, P. G., & Coppi, P. 2008, ApJ, 686, 1503
Bryan, G. L., & Norman, M. L. 1998, ApJ, 495, 80
Cen, R. 2014, ApJ, 781, 38
Chabrier, G. 2003, PASP, 115, 763
Cybulski, R., Yun, M. S., Fazio, G. G., & Gutermuth, R. A. 2014, MNRAS, 439, 3564
Dahlen, T., Mobasher, B., Faber, S. M., et al. 2013, ApJ, 775, 93
Darvish, B., Mobasher, B., Sobral, D., et al. 2016, ApJ, 825, 113
Darvish, B., Mobasher, B., Sobral, D., Scoville, N., & Aragon-Calvo, M. 2015, ApJ, 805, 121
Davies, L. J. M., Robotham, A. S. G., Driver, S. P., et al. 2016, MNRAS, 455, 4013
Fang, J. J., Faber, S. M., Koo, D. C., & Dekel, A. 2013, ApJ, 776, 63
Fillingham, S. P., Cooper, M. C., Pace, A. B., et al. 2016, MNRAS, 463, 1916
Fillingham, S. P., Cooper, M. C., Wheeler, C., et al. 2015, MNRAS, 454, 2039
Fossati, M., Wilman, D. J., Mendel, J. T., et al. 2017, ApJ, 835, 153
Galametz, A., Grazian, A., Fontana, A., et al. 2013, ApJS, 206, 10
Geha, M., Blanton, M. R., Yan, R., & Tinker, J. L. 2012, ApJ, 757, 85
Grogin, N. A., Kocevski, D. D., Faber, S. M., et al. 2011, ApJS, 197, 35
Guo, Y., Ferguson, H. C., Giavalisco, M., et al. 2013, ApJS, 207, 24
Guo, Y., Rafelski, M., Faber, S. M., et al. 2016, ApJ, 833, 37
Huang, J.-S., Faber, S. M., Willmer, C. N. A., et al. 2013, ApJ, 766, 21
Ilbert, O., McCracken, H. J., Le Fèvre, O., et al. 2013, A&A, 556, A55
Kawinwanichakij, L., Quadri, R. F., Papovich, C., et al. 2016, ApJ, 817, 9
Koekemoer, A. M., Faber, S. M., Ferguson, H. C., et al. 2011, ApJS, 197, 36
Lee, S.-K., Im, M., Kim, J.-W., et al. 2015, ApJ, 810, 90
Lin, L., Capak, P. L., Laigle, C., et al. 2016, ApJ, 817, 97
Momcheva, I. G., Brammer, G. B., van Dokkum, P. G., et al. 2016, ApJS, 225, 27
Muzzin, A., Marchesini, D., Stefanon, M., et al. 2013, ApJ, 777, 18
Nayyeri, H., Hemmati, S., Mobasher, B., et al. 2017, ApJS, 228, 7
Oke, J. B. 1974, ApJS, 27, 21
Peng, Y., Maiolino, R., & Cochrane, R. 2015, Natur, 521, 192
Quadri, R. F., Williams, R. J., Franx, M., & Hildebrandt, H. 2012, ApJ, 744, 88
Rodríguez-Puebla, A., Avila-Reese, V., Yang, X., et al. 2015, ApJ, 799, 130
Santini, P., Ferguson, H. C., Fontana, A., et al. 2015, ApJ, 801, 97
Scoville, N., Arnouts, S., Aussel, H., et al. 2013, ApJS, 206, 3
Skelton, R. E., Whitaker, K. E., Momcheva, I. G., et al. 2014, ApJS, 214, 24
Slater, C. T., & Bell, E. F. 2013, ApJ, 773, 17
Slater, C. T., & Bell, E. F. 2014, ApJ, 792, 141
Sparre, M., Hayward, C. C., Feldmann, R., et al. 2017, MNRAS, 466, 88
Tal, T., Dekel, A., Oesch, P., et al. 2014, ApJ, 789, 164
Tal, T., van Dokkum, P. G., Franx, M., et al. 2013, ApJ, 769, 31
Tinker, J. L., & Wetzel, A. R. 2010, ApJ, 719, 88
Weisz, D. R., Dolphin, A. E., Skillman, E. D., et al. 2015, ApJ, 804, 136
Wetzel, A. R., Tinker, J. L., Conroy, C., & van den Bosch, F. C. 2013, MNRAS, 432, 336
Wetzel, A. R., Tollerud, E. J., & Weisz, D. R. 2015, ApJL, 808, L27
Wheeler, C., Phillips, J. I., Cooper, M. C., Boylan-Kolchin, M., & Bullock, J. S. 2014, MNRAS, 442, 1396
Williams, R. J., Quadri, R. F., Franx, M., van Dokkum, P., & Labbé, I. 2009, ApJ, 691, 1879
Woo, J., Carollo, C. M., Faber, S. M., Dekel, A., & Tacchella, S. 2017, MNRAS, 464, 1077